CFAR DETECTION OF CHIRPLETS IN COLOURED GAUSSIAN NOISE

Gustavo López-Risueño, Jesús Grajal, Omar A. Yeste-Ojeda

Departamento de Señales, Sistemas y Radiocomunicaciones
ETSIT, Universidad Politécnica de Madrid
Ciudad Universitaria s/n, 28040 Madrid, Spain
risueno@gmr.ssr.upm.es

ABSTRACT

Two detectors based on the GLRT are presented to detect a chirplet in coloured Gaussian noise for known and unknown covariance structure, respectively. They are applied to detect multiple chirplets by atomic decomposition, which is modified to account for the operation conditions of both detectors. Both detectors are CFAR with respect to the noise power. The second one is CFAR with respect to the covariance structure as well.

1. INTRODUCTION

Detection of signals in complex environments keeping the false alarm probability constant despite changes or lack of knowledge about the background noise (clutter, jamming) is an important issue in radar and signal interception applications. Assuming stationarity within the signal frame under analysis, we propose two detectors based on atomic decomposition for zero-mean, circularly complex, coloured, Gaussian noise (**CCGN**) that extends a previous detector intended for complex white Gaussian noise (**CWGN**) [1]. The signal is modeled as a linear mixture of chirplets, which are used to model a wide variety of natural and man-made signals. Every chirplet

$$h_\gamma(n) = \left(\frac{\alpha}{\pi}\right)^{1/4} e^{-\frac{\alpha}{2}(n-T)^2} \cdot e^{j\left[2\pi f(n-T)+\pi\beta(n-T)^2\right]} , \quad (1)$$

is defined by a four-parameter vector $\boldsymbol{\gamma} = [\alpha, \beta, T, f]^{\mathrm{T}}$. α is inverse to the duration ($\sqrt{2/\alpha}$), β is the chirp rate, T and f are the mean time and frequency, respectively.

The first detector ($\mathbf{L_1}$) assumes known noise covariance structure and unknown power, and is based on the generalized maximum likelihood ratio test (GLRT) for only one chirplet in CCGN. The second detector ($\mathbf{L_2}$) assumes both unknown noise covariance structure and power and is inspired in the previous one. First of all, we present the structure of $\mathbf{L_1}$ and $\mathbf{L_2}$ for only one chirplet in CCGN and analyze their performance in terms of false alarm and detection probabilities. Their constant false alarm rate (CFAR) character is remarked. Then, the extension to the detection multichirplet signal with unknown number of components CCGN is carried out using atomic decomposition (**AD**), also known as matching pursuit [2].

AD is an adaptive approximation technique providing a sparse and meaningful representation of a wide range of signals by the use of a very redundant **dictionary** of functions called **atoms**. Let $D = \{\mathbf{h}_\gamma\}$ be the dictionary, and $\mathbf{x}$ the signal under analysis, the atoms of the signal expansion are usually obtained according to

$$\widehat{\gamma}_p = \arg\max_{\gamma} |\langle \mathbf{x_{p-1}}, \mathbf{h}_\gamma \rangle|^2 , \quad (2)$$

$$\widehat{b}_p = \langle \mathbf{x_{p-1}}, \mathbf{h}_{\widehat{\gamma}_p} \rangle , \quad (3)$$

$$\text{p-th residual: } \mathbf{x_p} = \mathbf{x_{p-1}} - \widehat{b}_p \mathbf{h}_{\widehat{\gamma}_p}, \ p = 1, 2, \ldots , \quad (4)$$

$$\mathbf{x_0} = \mathbf{x} .$$

This implementation features that the first extracted atom by AD is the maximum likelihood estimate (MLE) for one chirplet in CWGN [3]. Moreover, the detector for a multichirplet signal in CWGN applies the GLRT for a chirplet to every atom extracted by AD [1]. As the noise is coloured, we modify AD suitably so that the intimate relation to MLE is preserved. For every detector ($\mathbf{L_1}$ and $\mathbf{L_2}$) a new expression for AD is found. The validity of both schemes for multiple-chirplet detection is also illustrated by simulations.

2. DETECTION OF ONE CHIRPLET IN NOISE

For a chirplet in CCGN, the probability density functions for the well-known hypothesis testing problem are [1]

$$f_{H_0}(\mathbf{x}; \sigma, \mathbf{C}) = \frac{1}{(\pi\sigma^2)^N |\mathbf{C}|} \exp -\frac{\mathbf{x}^{\mathrm{H}} \mathbf{C}^{-1} \mathbf{x}}{\sigma^2} , \quad (5)$$

$$f_{H_1}\left(\mathbf{x}; \sigma, b, \gamma^{\mathrm{T}}, \mathbf{C}\right) = \frac{1}{(\pi\sigma^2)^N |\mathbf{C}|} \exp -\frac{(\mathbf{x} - b\mathbf{h}_\gamma)^{\mathrm{H}} \mathbf{C}^{-1} (\mathbf{x} - b\mathbf{h}_\gamma)}{\sigma^2} . \quad (6)$$

Signal $\mathbf{x}$ is the signal under analysis, and $b\mathbf{h}_\gamma$ the chirplet. $\mathbf{C}$ is the covariance structure and σ^2 the power of the noise. N is the signal length. Next, detectors $\mathbf{L_1}$ and $\mathbf{L_2}$ for only one chirplet are described.

This work was supported by CIDA and the National Board of Science and Technology (CICYT) under project TIC-2002-04569-C02-01

[1] H_0 is the null hypothesis (only noise), H_1 is the alternative one (a chirplet in noise).

2.1. Detection in CCGN with known structure

It can be proved from (6) that the MLE for the chirplet is

$$\widehat{\gamma} = \arg\max_{\gamma} \frac{\left|\mathbf{h}_{\gamma}^{\mathrm{H}}\mathbf{C}^{-1}\mathbf{x}\right|^2}{\mathbf{h}_{\gamma}^{\mathrm{H}}\mathbf{C}^{-1}\mathbf{h}_{\gamma}} , \quad (7)$$

$$\widehat{b} = \frac{\mathbf{h}_{\widehat{\gamma}}^{\mathrm{H}}\mathbf{C}^{-1}\mathbf{x}}{\mathbf{h}_{\widehat{\gamma}}^{\mathrm{H}}\mathbf{C}^{-1}\mathbf{h}_{\widehat{\gamma}}} , \quad (8)$$

These equations are similar to the atom extraction in usual AD (Eqs. 2, 3) taking into account the noise covariance structure, though. Additionally, the noise power MLE under H_0 becomes

$$\widehat{\sigma}^2_{H_0} = \frac{\mathbf{x}^{\mathrm{H}}\mathbf{C}^{-1}\mathbf{x}}{N} . \quad (9)$$

After some manipulations, the GLRT (denoted $\mathbf{L_1}$) becomes

$$\mathbf{L_1}(\mathbf{x}) = \frac{|\widehat{b}|^2\ \mathbf{h}_{\widehat{\gamma}}^{\mathrm{H}}\mathbf{C}^{-1}\mathbf{h}_{\widehat{\gamma}}}{\widehat{\sigma}^2_{H0}} = \frac{\left|\mathbf{h}_{\widehat{\gamma}}^{\mathrm{H}}\mathbf{C}^{-1}\mathbf{x}\right|^2}{\widehat{\sigma}^2_{H0}\ \mathbf{h}_{\widehat{\gamma}}^{\mathrm{H}}\mathbf{C}^{-1}\mathbf{h}_{\widehat{\gamma}}} \underset{H_0}{\overset{H_1}{\gtrless}} th . \quad (10)$$

Note that, for the particular case of CWGN, i.e. $\mathbf{C} = \mathbf{I}_N$, [2] the MLE from (7) results in the usual AD formulation (Eqs. 2, 3). Consequently, $\mathbf{L_1}$ becomes the GLRT for CWGN obtained in [1]. The particular detector for CWGN is denoted $\mathbf{L_0}$ in the sequel. $\mathbf{L_1}$ is CFAR with respect to the noise power and exhibits the same $\mathrm{P_{FA}}$ curve regardless of $\mathbf{C}$, as shown through simulations in Fig. 1.

2.2. Detection in CCGN with unknown covariance structure

In this case, the MLE for the pdf in (6) becomes ill-posed, since, unlike other similar approaches based on the Adaptive Matched Filter [4, 5], we do not have signal-free training data to estimate $\mathbf{C}$. Under hypothesis H_1, the MLE would lead to the $\mathbf{C}$ estimate

$$\widehat{\mathbf{C}}_{H_1} = \frac{1}{\widehat{\sigma}^2_{H_1}\ N}\ \left(\mathbf{x} - \widehat{b}\mathbf{h}_{\widehat{\gamma}}\right)\ \left(\mathbf{x} - \widehat{b}\mathbf{h}_{\widehat{\gamma}}\right)^{\mathrm{H}} , \quad (11)$$

which is a rank-one matrix. Thus, the inverse does not exist and cannot be replaced in (6). The problem may be regularized constraining the MLE in the subset of Toeplitz, Hermitian matrices, but the optimization problem does not have analytical solution, and the search space is highly dimensional [3] to be solved numerically.

We propose an efficient algorithm inspired by the previous detector $\mathbf{L_1}$ that estimates the chirplet parameters and the covariance structure by an iterative procedure. The algorithm splits the estimation problem into two steps. The first step estimates the chirplet and the second one the covariance structure $\mathbf{C}$. The procedure is iterated to improve the estimation of both the chirplet and $\mathbf{C}$. At every iteration, Eq. (7) of $\mathbf{L_1}$ could be used with the $\mathbf{C}$ estimate from the previous iteration. However, it would required the inversion of the $\mathbf{C}$ estimate. We filter the signal by means of a whitening filter estimate instead. Both inverse-of-$\mathbf{C}$ and whitening-filter approaches are equivalent: The former looks at the signal samples as a random vector and the latter as a stochastic process. To attain high efficiency, autoregressive (AR) modeling is utilized, so that the Prediction Error Filter becomes the desired whitening filter [6]. The algorithm works as follows

Step 0: $\mathcal{F}^{(0)}$ = Filter with impulse response $\delta(n)$

Step 1:
$$\widehat{\gamma}^{(i+1)} = \arg\max_{\gamma} \frac{\left|\left(\mathcal{F}^{(i)}(\mathbf{h}_{\gamma})\right)^{\mathrm{H}}\ \mathcal{F}^{(i)}(\mathbf{x})\right|^2}{\left\|\mathcal{F}^{(i)}(\mathbf{h}_{\gamma})\right\|^2} \quad (12)$$

$$\widehat{b}^{(i+1)} = \frac{\left(\mathcal{F}^{(i)}\left(\mathbf{h}_{\widehat{\gamma}^{(i+1)}}\right)\right)^{\mathrm{H}}\ \mathcal{F}^{(i)}(\mathbf{x})}{\left\|\mathcal{F}^{(i)}\left(\mathbf{h}_{\widehat{\gamma}^{(i+1)}}\right)\right\|^2} , \quad (13)$$

Step 2: $\mathcal{F}^{(i+1)}$ = Prediction Error Filter by AR modeling of $\mathbf{x} - \widehat{b}^{(i+1)}\mathbf{h}_{\widehat{\gamma}^{(i+1)}}$.
Goto Step 1 unless termination

Termination occurs when the change in the chirplet estimate from an iteration to the next one is below a threshold. Operator $\mathcal{F}^{(i)}$ is the Prediction Error Filter computed at the i-th iteration. The operation $\mathcal{F}^{(i)}(\mathbf{s})$ means filtering of signal $\mathbf{s}$. To initialize, $\mathcal{F}^{(0)}$ assumes white noise. The AR model and, therefore, the Prediction Error Filter are computed by the Burg's method [6] due to its numerical stability and its recursive implementation. At every iteration the AR order is optimum according to the Akaike's Final Predictor Error [7]. Any stationary process with continuous spectral density can be written as a unique AR model [8], so that the proposed method is general. For some processes requiring AR models of order ∞, such as Moving Average (MA) ones, a loss in performance may be expected since the AR order is upper-bounded for practical reasons. However, the algorithm works without appreciable losses.

Final values in the optimization process are represented without superscript: $\mathcal{F}$, $\widehat{\gamma}$, $\widehat{b}$, and the detector becomes

$$\mathbf{L_2}(\mathbf{x}) = \frac{\left|\left(\mathcal{F}(\mathbf{h}_{\widehat{\gamma}})\right)^{\mathrm{H}}\ \mathcal{F}(\mathbf{x})\right|^2}{\widehat{\sigma}^2_{H_0}\ \left\|\mathcal{F}(\mathbf{h}_{\widehat{\gamma}})\right\|^2} \underset{H_0}{\overset{H_1}{\gtrless}} th , \quad (14)$$

$$\widehat{\sigma}^2_{H_0} = \frac{\left\|\mathcal{F}(\mathbf{x})\right\|^2}{N} . \quad (15)$$

$\mathbf{L_2}$ is CFAR with respect to the covariance structure and the noise power, as shown through simulations in the next section.

3. PERFORMANCE ANALYSIS

The section is devoted to the analysis of detectors $\mathbf{L_1}$ and $\mathbf{L_2}$ in the monochirplet case by simulation. For the optimization in Eqs. (7) and (12), a genetic algorithm refined by a Quasi-Newton method is used. This algorithm is described in [1, Table 1]. The number of samples (N) is 1024.

3.1. False Alarm Probability

Fig. 1 shows the $\mathrm{P_{FA}}$ of both $\mathbf{L_1}$ and $\mathbf{L_2}$ simulated for different covariance structures $\mathbf{C}$: white, 1st-order AR, 1st-order

[2] $\mathbf{I}_N$ is the N-identity matrix

[3] Dimension $N + 4 + 2$: 4 is the dimension of the chirplet parameter vector $\boldsymbol{\gamma}$, and 2 refers to the chirplet coefficient b, which is complex.

MA, and 2nd-order AR noises. For AR noises, the poles (pi) are written in the legend. For MA noises, the zeros (zi). Two important properties arise: 1) for $\mathbf{L_1}$, the false alarm probability (P_{FA}) curve is independent of $\mathbf{C}$, and 2) $\mathbf{L_2}$ is CFAR with respect to $\mathbf{C}$. Theoretical proof of these two properties is under investigation. Both detectors are CFAR with respect to the noise power, since Eqs. (7), (10), (12), and (14) are scale invariant. [4]

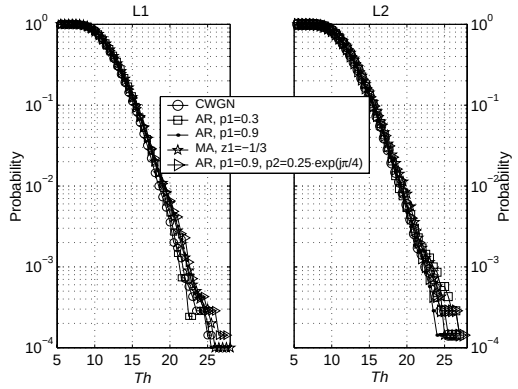

Fig. 1. P_{FA} vs. threshold of $\mathbf{L_1}$ (left) and $\mathbf{L_2}$ (right).

3.2. Detection Probability

Detection performance of $\mathbf{L_1}$ and $\mathbf{L_2}$ is summarized through results obtained for three chirplets, denoted $\boldsymbol{\gamma_1}$, $\boldsymbol{\gamma_2}$ and $\boldsymbol{\gamma_3}$, whose parameters are: $\boldsymbol{\gamma_1} = \left[10^{-3}, 3\ 10^{-3}, 500, 0.25\right]$, $\boldsymbol{\gamma_2} = \left[10^{-3}, 0, 500, 0.25\right]$ and $\boldsymbol{\gamma_3} = \left[10^{-3}, 3\ 10^{-3}, 500, 0.0714\right]$. We use the Energy-to-Noise Ratio (**ENR**) instead of the SNR, since ENR does not depend on the chirplet parameters [1]. ENR is defined as $|b|^2/\sigma^2$, with $|b|^2$ the chirplet energy and σ^2 the noise power.

The sensitivity of the detectors is plotted in Fig. 2 for several 1st-order AR processes. The correlation coefficient ρ (it is equal to the pole value in this case) between two successive samples is used in the horizontal axis. The sensitivity is defined as the minimum ENR attaining $Pd = 90\%$ at $P_{FA} = 10^{-6}$. Detector $\mathbf{L_0}$ (intended for white noise) is also tested. $\mathbf{L_1}$ performs better than $\mathbf{L_2}$, as $\mathbf{L_2}$ has to estimate the covariance structure. In general, $\mathbf{L_1}$ and $\mathbf{L_2}$ outperform $\mathbf{L_0}$, since $\mathbf{L_0}$ assumes white noise. However, $\mathbf{L_0}$ turns out to be better if the noise and the chirplet are close in the time-frequency plane ($\boldsymbol{\gamma_3}$ with both $\mathbf{L_1}$ and $\mathbf{L_2}$). Except for this situation, the general rule-of-thumb is that the further the noise and chirplet are in the time-frequency plane, the better the sensitivity becomes. For $\mathbf{L_0}$, the sensitivity does not depend on the chirplet duration (α), as in the presence of white noise [1].

As for the termination condition in $\mathbf{L_2}$ (Eqs. 12 and 13), after two iterations, low error is achieved. As an example, Fig. 3 shows the root mean squared errors (RMSE) of the α estimate of chirplet $\boldsymbol{\gamma_1}$ in a 1st-AR noise with $\rho = 0.9$ for several ENR's. The RMSE in the estimation of the AR parameters (AR parameters considered as a vector) is also plotted. Clearly, the RMSE does not change from the 2nd iteration on. The rest of the chirplet parameters present similar behavior. Although not shown, the mean order becomes close to one (the true order) from the 2nd iteration on.

The detection of $\boldsymbol{\gamma_2}$ with $\mathbf{L_2}$ exhibits a relatively low performance due to the proper philosophy of $\mathbf{L_2}$: For low ENR, Eq. (12) in **step 1** does not estimate the true chirplet because the global optimum is due to the noise. Then **step 2** not only models by AR modeling the noise but also the signal and, in the next estimation, the filter $\mathcal{F}^{(i)}$ tries to remove not only the noise but also the signal. If the chirplet has chirp rate, the order required to estimate the AR model of both signal and noise is high. On the contrary, for $\beta = 0$, the required order is low. For practical reasons, the AR order is constrained up to 10. Therefore, the AR model includes both signal and noise for zero-β chirplets. $\mathcal{F}^{(i)}$ affects both of them, and the signal cannot be estimated at the next iteration. For nonzero β, the AR model cannot include the signal suitably since a higher order would be required. Then, $\mathcal{F}^{(i)}$ mainly affects the noise. The problem disappears at high ENR, since (12) estimates the true chirplet at the first iteration. For illustrative purposes, the Pd curve is shown in Fig 4 for $\boldsymbol{\gamma_2}$ in a 1st-order AR noise with $\rho = 0.9$. At very low ENR, Pd rises up because the AR modeling does not include the signal, which is negligible regarding the noise, and $\mathcal{F}^{(i)}$ mainly affects the noise.

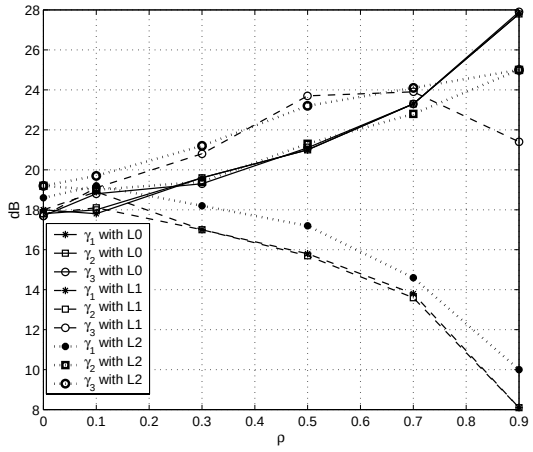

Fig. 2. Sensitivity (dB) for $\mathbf{L_1}$, $\mathbf{L_2}$ and $\mathbf{L_0}$. ($Pd = 90\%$, $P_{FA} = 10^{-6}$)

4. MULTICOMPONENT DETECTOR

Detectors $\mathbf{L_1}$ and $\mathbf{L_2}$ obtained in the monochirplet case are extended to multichirplet signals using AD as in [1] for CWGN. We use multi-$\mathbf{L_i}$ and mono-$\mathbf{L_i}$ to distinguish between the multicomponent algorithm and that intended for only one chirplet. The usual AD is modified to take into account the noise correlation. For multi-$\mathbf{L_1}$, AD is obtained by (7), and (8). Mono-$\mathbf{L_1}$ is then applied to the extracted atom. Once the p-th atom is extracted, the p-th residual is computed as in (4) and the extractions carry on. Similarly,

[4] Ideal behavior of the optimization algorithm in Eqs. (7), (12) is assumed.

for multi-$\mathbf{L_2}$, AD extracts the atoms using the iterative procedure from (12) and (13). Every extracted atom undergoes then detector mono-$\mathbf{L_2}$. In general, mono-$\mathbf{L_i}$'s use the same threshold regardless of the extraction order. Additionally, the AD stopping criterion for multi-$\mathbf{L_i}$ consists of 4 successive atoms without passing the mono-$\mathbf{L_i}$'s. This is necessary mainly due to the probabilistic behavior of the employed genetic algorithm. For multi-$\mathbf{L_i}$, the P_{FA} is defined as the probability that at least one atom surpasses the mono-$\mathbf{L_i}$ tests when there is only noise. In terms of P_{FA}, multi- $\mathbf{L_1}$ and $\mathbf{L_2}$ exhibit the same CFAR properties as mono-$\mathbf{L_1}$ and $\mathbf{L_2}$ in section 3. The thresholds change with respect to one chirplet in noise, as the stopping criterion involves more than one extraction.

A signal with three chirplets is studied. The first component is chirplet $\boldsymbol{\gamma_1}$. The second one is $\boldsymbol{\gamma_4}$ ($\alpha = 10^{-4}$, $\beta = -10^{-3}$, $T = 500$, $f = 0.25$). The third one is $\boldsymbol{\gamma_5}$ ($\alpha = 10^{-3}$, $\beta = 0$, $T = 150$, $f = 0.25$). The adaptive spectrogram [2] of the multichirplet signal is shown in Fig. 5. The noise is a 1st-order AR process with pole 0.9. For multi-$\mathbf{L_1}$, initially, the individual ENRs are 8.1, 11.5, 21.4 dB, respectively, and assure $Pd = 90\%$ using mono-$\mathbf{L_1}$ when they are alone. For multi-$\mathbf{L_2}$, they are 10, 20 and 25 dB. The initial ENR values are changed by adding the same increase to build the curves of Pd for each chirplet in Fig. 6. In the legend, *mono* means the monocomponent detection for a monochirplet signal (only the first extraction), and *multi* the multicomponent detection of the multichirplet signal. The multi-$\mathbf{L_i}$'s are tested not only for the multichirplet signal but also when the signal is made of only one chirplet ($\boldsymbol{\gamma_1}$, $\boldsymbol{\gamma_4}$ or $\boldsymbol{\gamma_5}$). The Pd curves for both cases are similar. The multi-$\mathbf{L_i}$ Pd is greater than the mono-$\mathbf{L_i}$ (only the first extraction) since the multi-$\mathbf{L_i}$ performs more extractions (the stopping criterion).

The previous example shows the good performance of multi-$\mathbf{L_1}$ and $\mathbf{L_2}$. However, if there are several chirplets with zero β, multi-$\mathbf{L_2}$ may not detect some of them due to the same reasons argued for the loss in performance for chirplet $\boldsymbol{\gamma_2}$ (section 3). The solution of this problem is still under investigation.

5. CONCLUSION

Two detectors for mono- and multichirplet detection in correlated Gaussian noise have been presented. The first one assumes known covariance structure and is based on the GLRT for only one chirplet. The second one assumes unknown covariance structure, and utilizes an iterative two-step estimation algorithm that includes AR modeling to increase the efficiency. The first one is CFAR with respect to the noise power and the P_{FA} curve does not depend on the covariance structure. The second one is CFAR with respect to both the noise power and the covariance structure, and does not require the use of signal-free training data unlike other approaches.

6. REFERENCES

[1] G. López-Risueño and J. Grajal, "Unknown Signal Detection via Atomic Decomposition," in *IEEE SSP*, 2001.

[2] S. Mallat, *A Wavelet Tour of Signal Processing*, Academic Press, 1998.

[3] J. C. O'Neill and P. Flandrin, "Chirp Hunting," in *IEEE TFTS*, 1998.

[4] F.C. Robey, D.R. Fuhrman, E.J. Kelly, and R. Nitzberg, "A CFAR Adaptive Matched Filter Detector," *IEEE Trans. AESS*, vol. AESS-28, 1992.

[5] S. Kraut, L.L. Scharf, and L.T. McWhorter, "Adaptive Subspace Detectors," *IEEE Trans. SP*, vol. SP-49, 2001.

[6] S. Haykin, *Adaptive Filter Theory*, Prentice Hall, 3rd edition, 1996.

[7] M.B. Priestley, *Spectral Analysis and Time Series*, Academic Press, 1981.

[8] P.M.T. Broersen, "Facts and Fiction in Spectral Analisys," *IEEE Trans. IM*, vol. IM-49, 2000.

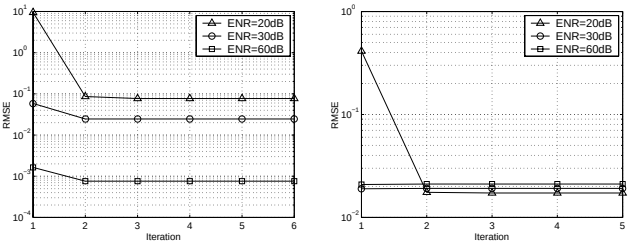

Fig. 3. Estimation error vs. iterations for $\mathbf{L_2}$. Noise is a 1-st order AR process with pole 0.9.

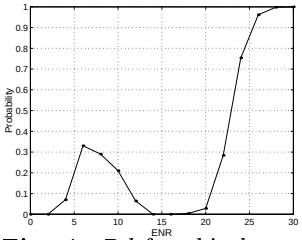

Fig. 4. Pd for chirplet $\boldsymbol{\gamma_2}$ with $\mathbf{L_2}$.

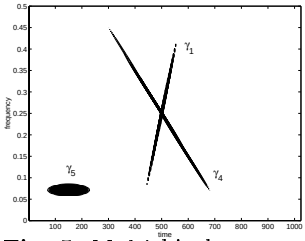

Fig. 5. Multichirplet example: Adaptive Spectrogram.

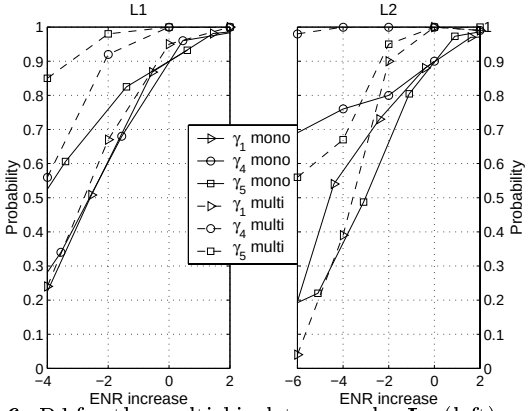

Fig. 6. Pd for the multichirplet example. $\mathbf{L_1}$ (left) and $\mathbf{L_2}$ (right). $P_{FA} = 10^{-6}$.